

www.acsnano.org

Continuous Curvature Change into Controllable and Responsive Onion-like Vesicles by Rigid Sphere—Rod Amphiphiles

Jiancheng Luo, Tong Liu, Kun Qian, Benqian Wei, Yinghe Hu, Min Gao, Xinyu Sun, Zhiwei Lin, Jiahui Chen, Mrinal K. Bera, Yuhang Chen, Ruimeng Zhang, Jialin Mao, Chrys Wesdemiotis, Mesfin Tsige, Stephen Z. D. Cheng,* and Tianbo Liu*



Cite This: ACS Nano 2020, 14, 1811–1822



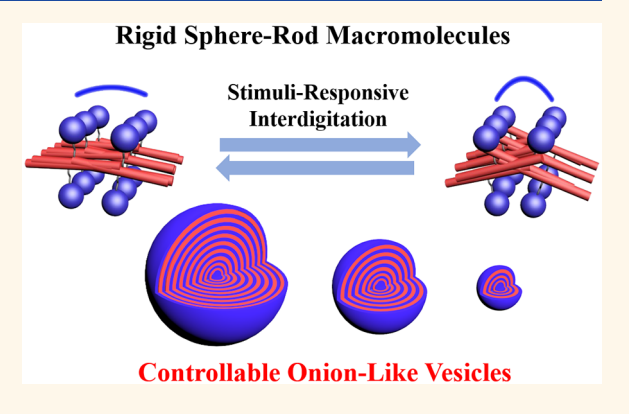
ACCESS

III Metrics & More

Article Recommendations

SI Supporting Information

ABSTRACT: We observe the formation of highly controllable and responsive onion-like vesicles by using rigid sphere—rod amphiphilic hybrid macromolecules, composed of charged, hydrophilic Keggintype clusters (spheres) and hydrophobic rod-like oligofluorenes (OFs). Unlike the commonly used approach, which mainly relies on chain bending of flexible molecules to satisfy different curvatures in onion-like vesicles, the rigid hybrids form flexible interdigitations by tuning the angles between OFs, leading to the formation of bilayers with different sizes. The self-assembled vesicles possess complete onion-like structures from most inner to outer layers, and their size (layer number) can be accurately manipulated by different solution conditions including solvent polarity, ionic strength, temperature, and hybrid concentration, with fixed interbilayer distance under all conditions. Moreover, the vesicle size (layer number) shows excellent



reversibility to the change of temperature. The charged feature of spheres, rod length, and overall hybrid architecture shows significant effects on the formation of such onion-like vesicles.

KEYWORDS: continuous curvature change, onion-like vesicles, rigid amphiphilic macromolecules, sphere-rod geometry, stimuli-responsive nanostructures

ormed by amphiphilic molecules such as phospholipids and block copolymers, vesicles are one of the most fundamental nanostructures in natural and artificial processes.¹⁻³ Over the past decades, the vesicular structures have shown attractive properties and drawn much attention in various fields such as supramolecular chemistry, 4-7 chemical reaction, 8,9 imaging, 10 and simulation. 11-13 In addition to common hollow vesicles (with one bilayer membrane), amphiphiles are also found to form interesting onion-like vesicles (multilayered vesicles) which consist of concentric alternating bilayers, and the observations of onion-like vesicles have been extensively reported in various systems including small-molecule surfactants, 14-17 block copolymers, 18-21 dendrimers, 22-27 surfactant-encapsulated complexes, 28 and clusterbased hybrids²⁹⁻³³ and also elucidated by simulations.^{34,35} Although the formation of onion-like vesicles can enrich supramolecular structures in amphiphilic systems, a microscopic mechanism to reveal their self-assembly process is still not fully understood, especially, why some amphiphiles can

form onion-like vesicles while others cannot. Additionally, the size of onion-like vesicles and their layer number are usually difficult to control and exhibit significant polydispersity in solution. Therefore, a well-defined system with controllable molecular composition/architecture could provide a better fundamental understanding about the scope and limitation of amphiphilic molecules during their self-assembly process.

Two basic requirements are preferred to achieve onion-like vesicles: (1) Flexible amphiphilic molecules. The molecules need to tolerate a broad range of curvature changes from inner to outer layers, which requires them to undergo various and continuous degrees of chain bending or conformational change to satisfy different curvatures. Therefore, onion-like vesicles are

Received: September 25, 2019 Accepted: January 29, 2020 Published: January 29, 2020



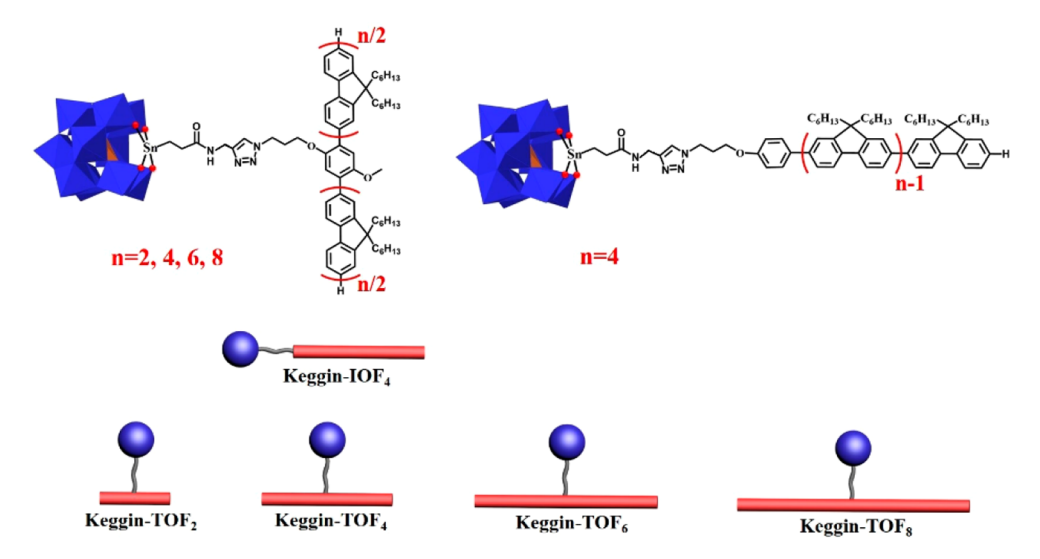


Figure 1. Chemical structures and simplified molecular models of sphere-rod shaped hybrids. The blue spheres represent hydrophilic Keggin clusters, and the red rods represent hydrophobic OFs.

often observed in flexible amphiphilic molecules such as dendrimers and polymers. If molecules are not flexible enough, they cannot be significantly bent to form inner layers (large curvature). Accordingly, the self-assembled vesicles might have only a few outer layers rather than the complete onion-like structures. (2) Strong interbilayer attraction. The onion-like vesicles are formed by layer-by-layer self-assembly of differently sized bilayers. If the attraction between bilayers (hydrophilic domains if in polar solvents) is too weak in solution, the bilayers cannot stay closely within a certain distance to each other, leading to the formation of regular hollow vesicles.

In the literature, the commonly used approach to satisfy the large range of continuous curvature change is to increase the flexibility of molecules (e.g., long polymer chains 18 or dendrimers²²). However, it is still difficult to achieve uniform, highly controllable/responsive onion-like vesicles by flexible amphiphiles in most cases, largely due to the very energyconsuming bending process of the flexible molecules in different bilayers (especially for the inner bilayers).36-38 In this work, we report the discovery of uniform, well-controlled onion-like vesicles in solutions of rigid amphiphilic hybrids with special sphere-rod geometry: the charged, hydrophilic, spherical Keggin-type clusters and hydrophobic, rod-like oligofluorenes (OFs) with different OF lengths and overall hybrid architectures. The incorporation of OFs renders an amphiphilic feature of the hybrid molecules in polar solvents, and the competition between the electrostatic interaction (from Keggins) and the hydrophobic interaction (from OFs) is expected to be critical for their self-assembly. 39,40 Both components are very rigid, which distinguishes them from soft amphiphiles such as block copolymers. The Keggin clusters are typical macroions whose solution behaviors are heavily controlled by the counterion-mediated electrostatic interaction. 41 The unique sphere-rod geometry makes these hybrids nice models to understand the correlation between the molecular shape and their self-assembly behaviors. While we might speculate before that the rigid components would limit the versatility of self-assembled structures formed by such "block copolymers", we show here that these special amphiphiles actually can demonstrate unexpected exciting phenomena in solution. The study also represents an attempt

to explore almost uncharted self-assembly behavior of rigid block copolymers. While the flexible block copolymers have been extensively studied in the past decades, ⁴² and the rigid–flexible block copolymers have also drawn considerable attention, ^{43–46} studies of fully rigid block copolymers are still scarce.

RESULTS AND DISCUSSION

Synthesis of Sphere-Rod Amphiphilic Hybrids and Their Molecular Structures. The Keggin-type polyoxometalate clusters and oligofluorenes with different lengths were chemically linked to form sphere-rod shaped hybrids (Figure 1). The alkyne-functionalized Keggins (4⁻ charge) balanced by tetrabutyl ammonium counterions (TBAs) were synthesized based on the reported method,⁴⁷ and the azide-containing OFs were synthesized from step-by-step addition of fluorene repeating units as in our previous work. 48,49 Following the postfunctionalization approach, 50,51 two components were successfully coupled by using azide-alkyne Huisgen cycloaddition (detailed procedures in the Supporting Information). Two sets of hybrid molecules were obtained: (1) T-shaped hybrids with various rod lengths (Keggin-TOF_n, n = 2, 4, 6, 8); (2) with the same rod length as Keggin-TOF₄, but the Keggins were connected to the center of OFs to create an Ishaped hybrid architecture (Keggin-IOF₄). All the products were characterized by ¹H NMR, matrix-assisted laser desorption/ionization-time-of-flight mass spectrometry (MALDI-TOF MS), Fourier-transform infrared spectroscopy (FTIR), and UV-vis spectroscopy, shown in Figures S2-S17.

Self-Assembly of Onion-like Vesicles in Solution of Keggin–TOF₄. With the hydrophilic Keggin clusters and hydrophobic OFs, the hybrid molecules are expected to be amphiphilic and show self-assembly behaviors in selective solvents. 40,42,52,53 The Keggin–TOF₄ hybrids are quite soluble in acetonitrile (MeCN) but insoluble in water. Water/acetonitrile mixed solvents are chosen to trigger the self-assembly. After sample preparation, very high scattered intensity is recorded by static light scattering (SLS) measurements from 0.2 mg/mL Keggin–TOF₄ solutions when water content ranges from 50% to 85%, indicating the formation of large self-assembled structures. When the water content is

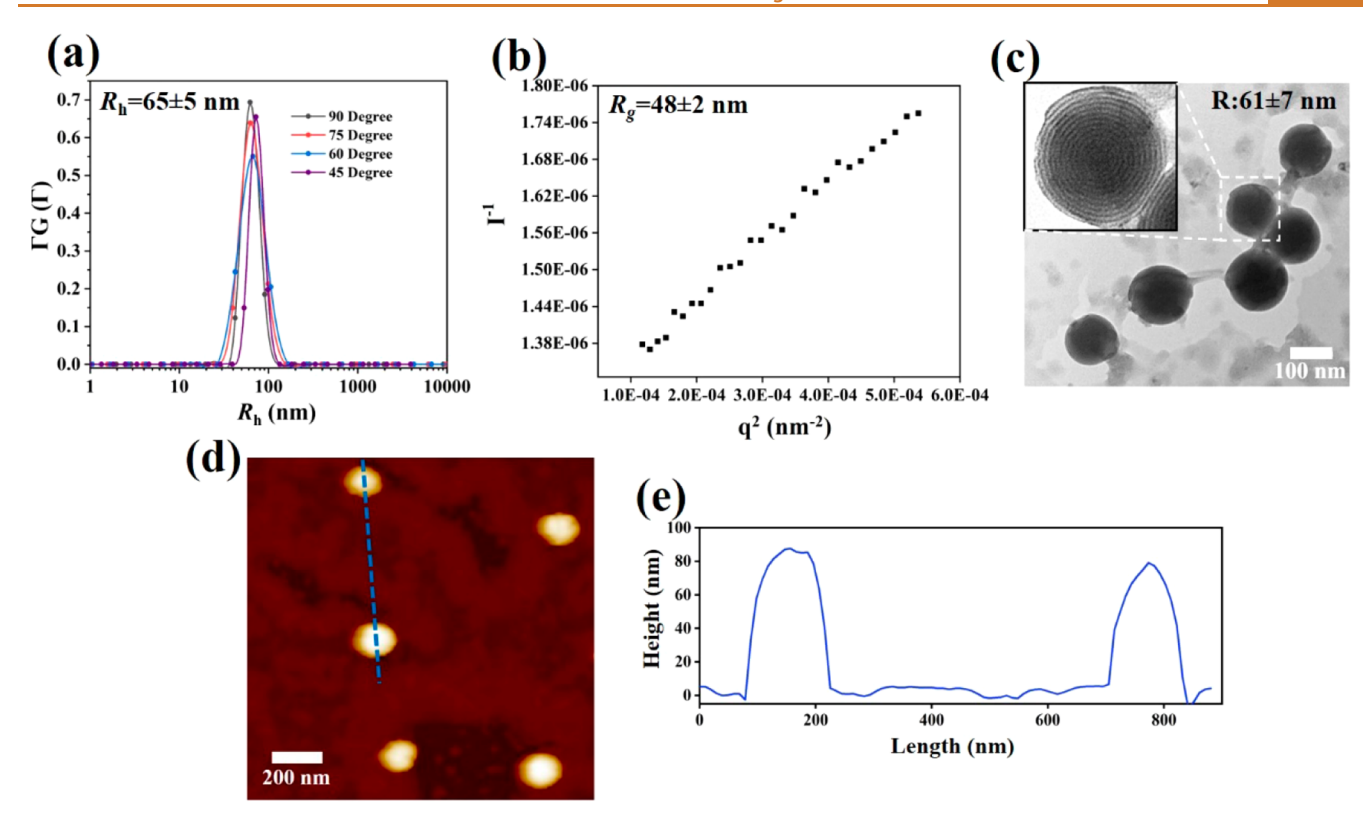


Figure 2. (a) CONTIN analysis of DLS results from 0.2 mg/mL Keggin-TOF $_4$ in 50% water/MeCN solutions. (b) SLS measurements from 0.2 mg/mL Keggin-TOF $_4$ in 50% water/MeCN solutions; the $R_{\rm g}$ value is obtained by linear fitting. (c) TEM images of spherical assemblies obtained from 0.2 mg/mL Keggin-TOF $_4$ in 50% water/MeCN. The onion-like structures can be clearly observed in the zoomed-in image. (d) AFM characterization of spherical assemblies obtained from 0.2 mg/mL Keggin-TOF $_4$ in 50% water/MeCN. (e) Height profile measured from blue dashed line.

below 45%, the solutions show very low scattered intensity close to the solvent level, suggesting that the hybrids stay as soluble individual molecules. Obvious precipitation is observed at a water content of >90%. A typical CONTIN analysis⁵⁴ of dynamic light scattering (DLS) measurements from 50% water/MeCN solutions shows that the average hydrodynamic radius (R_h) of assemblies is 65 \pm 5 nm and angular independent (Figure 2a), suggesting spherical morphology of assemblies in solution. The radius of gyration (R_g) of the large assemblies obtained from SLS measurements is 48 ± 2 nm (Figure 2b), leading to an R_g/R_h ratio of 0.74, close to the theoretical value for a solid sphere (0.77).55 Atomic force microscopy (AFM) measurements also show the spherical feature of the assemblies and the average height of spheres (Figure 2d,e) is 82 ± 6 nm, which again confirms that the selfassembled structures are likely to be solid rather than hollow spheres. Moreover, typical transmission electron microscopy (TEM) images show that the average radius of the spheres is 61 ± 7 nm (Figure 2c), nicely matching the R_h value from DLS measurements. The size distribution of spherical assemblies is quite narrow compared with those from vesicles and liposomes in the literature. 36,57 Interestingly, a zoom-in TEM image reveals that these solid spheres have strict onion-like structures: concentric spheres from the core to outer layers. The combined results show that narrow distributed onion-like vesicles have been formed in a solution of Keggin-TOF₄.

Mechanism of Bilayer Formation and Layer-by-Layer Assembly in Onion-like Vesicles. It is intriguing why the rigid sphere—rod hybrids tend to form onion-like vesicles, as in such structures the curvatures of different bilayers vary in a

very broad range. From the molecular structure of Keggin-TOF₄, the dimension of the TOF₄ rod length (3.4 nm) is considerably larger than the diameter of the Keggins (1.0 nm). Accordingly, in order to form onion-like structures, a long distance between Keggins must exist in the bilayers if the TOF₄ rods are not interdigitated with each other (model B in Figure 3a), which makes the bilayer structure unstable, and it is difficult to achieve continuously variable curvatures. Therefore, we speculate that the TOF4 rods will be significantly interdigitated with each other to form a more compact packing (model A in Figure 3a), and the adjustment of interdigitation angle will satisfy curvature change for vesicles at different layers. To verify this, the 2D nuclear Overhauser effect spectroscopy (NOESY) NMR technique was applied to study spatial arrangements of the TOF4 rods in bilayers. Generally, the NOE signal between two protons depends on their spatial distance (r), and its strength is proportional to $1/r^{6.58,59}$ Consequently, the NOE signal between two protons can be observed within a very short distance only (<5 Å). From the molecular structure, the distance between center and end of the TOF₄ is ca. 1.5 nm (Figure 3c), which is much longer than the detection limit for NOESY signal, and this length will not change significantly during self-assembly due to the rigid nature of the TOF4 rod, ruling out the possibility that the center-to-end NOE signals are contributed from intramolecular correlation within one hybrid molecule. As a result, the NOESY technique can distinguish whether the interdigitation between adjacent TOF4 rods has been formed in bilayers. If no interdigitation is formed (model B), the centerto-end distance is still out of the detection limit for NOE

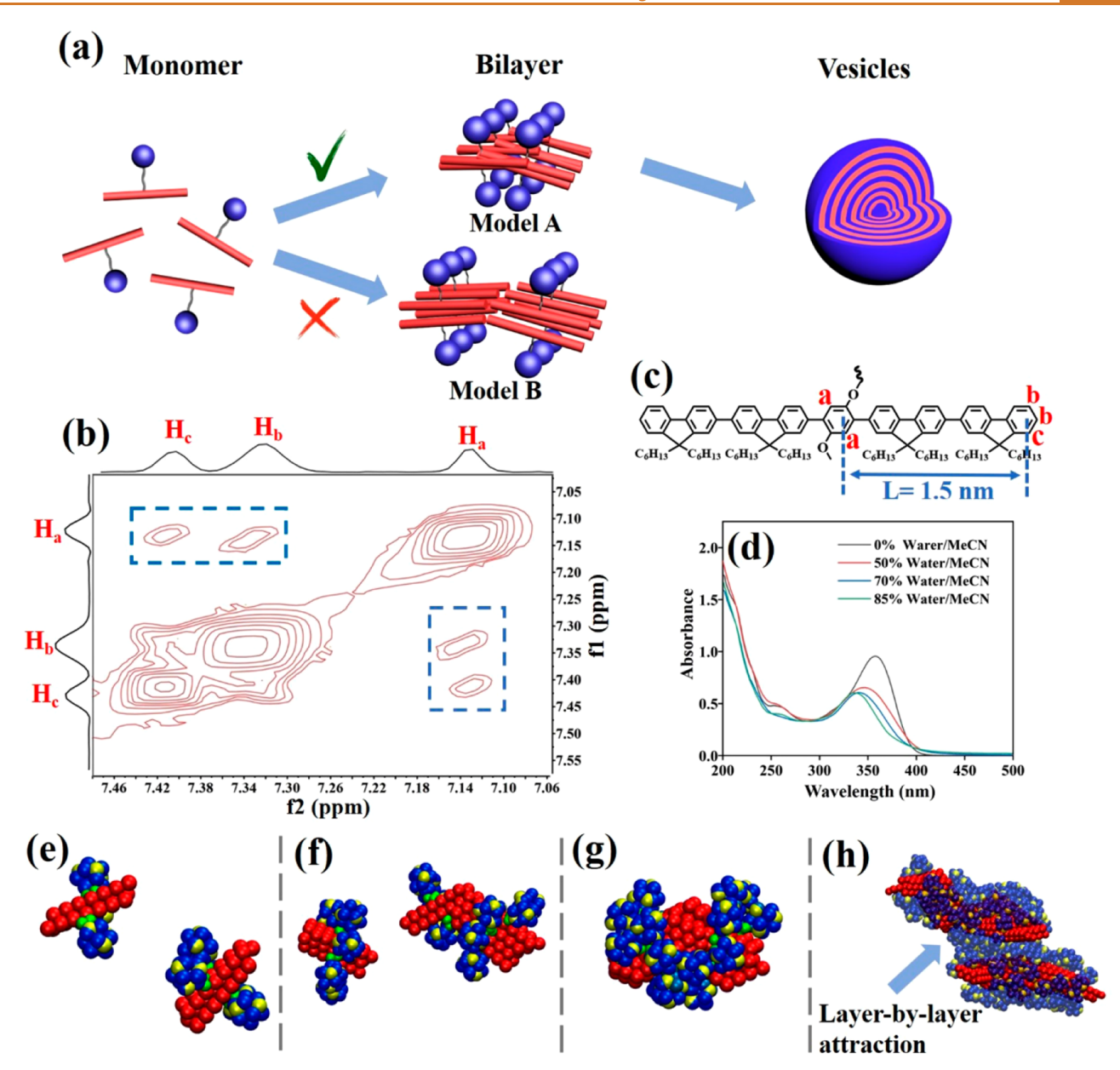


Figure 3. (a) Schematic illustration to show the model of bilayers. (b) 2D NOESY spectra from onion-like vesicle solutions. The negative correlation peaks are highlighted in the dashed blue rectangle. (c) Chemical structure of TOF_4 rods and assignments of different protons. (d) Comparison of UV-vis spectra before (0% water/MeCN) and after (50–85% water/MeCN) the formation of onion-like vesicles. Snapshots of CG simulation at (e) 10 ns, (f) 40 ns, (g) 70 ns, and (h) 300 ns. Color code: blue (Keggin), red (OF), green (linker), yellow (charge). The transparence of the blue spheres in (h) has been adjusted for clarity.

signal. On the other hand, significant intermolecular overlap (model A) between the TOF_4 rods can lead to a close centerto-end distance as well as the appearance of NOE signal. Based on the 1D 1H NMR spectra (Figure S4) of Keggin– TOF_4 hybrid in single molecular state, the proton from the center of the TOF_4 rods is assigned as H_a , and the protons from the end of the TOF_4 rods are assigned as H_b and H_c (Figure 3c), respectively. After the formation of onion-like vesicles, several sets of negative NOE cross peaks appear (full spectra in Figure S18), indicating the strong spatial interaction between hybrid molecules. Importantly, zoomed-in spectra from the aromatic region clearly show the NOE peaks from H_a – H_b and H_a – H_c (highlighted in Figure 3b), that is, the correlation between the center and the end of TOF_4 rods. This strongly suggests that a very close spatial distance (<5 Å) between H_a of one TOF_4 rod

and H_b/H_c of another nearby TOF_4 rod (intermolecular correlation) is formed after self-assembly, which consequently confirms our speculation that the TOF_4 rods will be significantly interdigitated in bilayers (model A). Additionally, UV—vis spectra (Figure 3d) show that the absorbance peaks from TOF_4 rods have obvious wavelength shifts after self-assembly, indicating that the conjugation degree of TOF_4 rods has been affected due to the close inter-rod distance. 60,61

Previously, our group reported that the counterion-mediated electrostatic attraction had very important contributions to the solution behavior of hydrophilic, charged polyoxometalate clusters (POMs). The attraction is strong enough to overcome the electrostatic repulsion between like-charged clusters and consequently brings them together. Therefore, we speculate that the charged Keggins have a significant influence

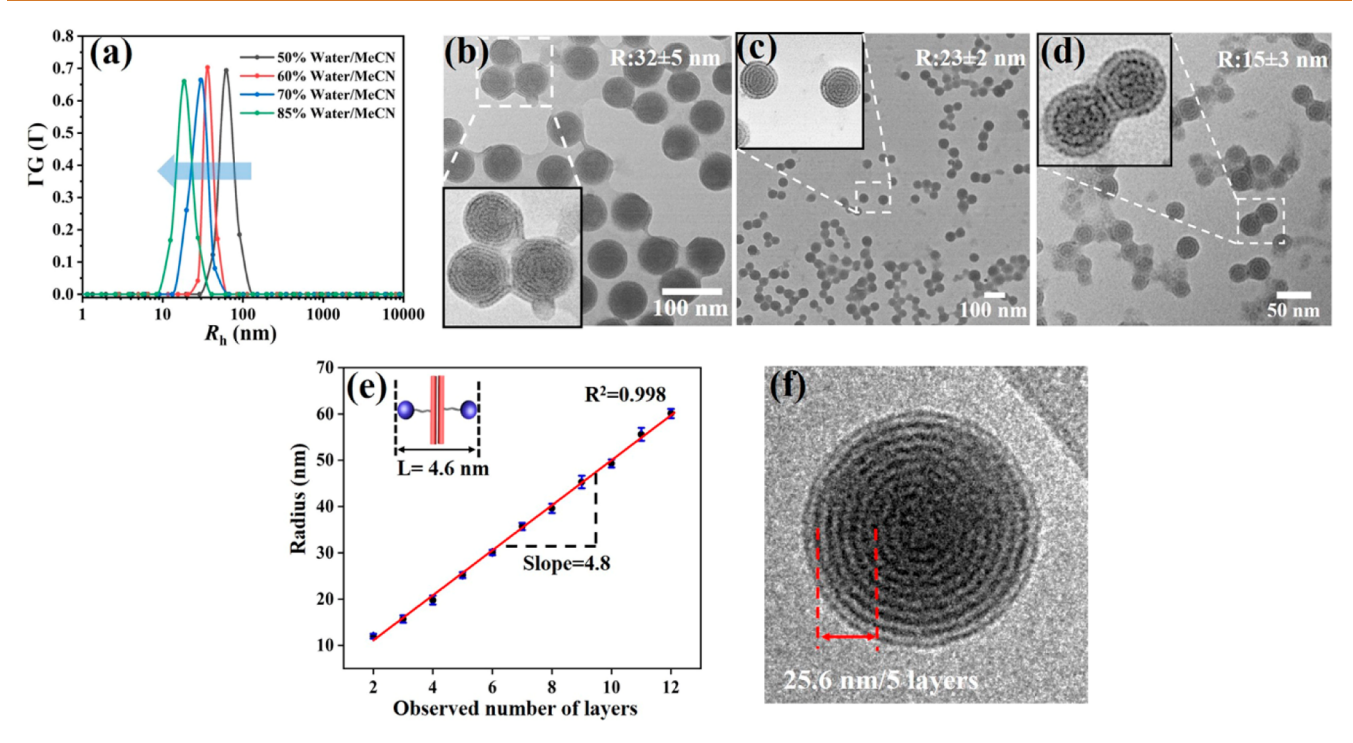


Figure 4. (a) CONTIN analysis of 0.2 mg/mL Keggin-TOF₄ prepared in different solvent combinations. TEM images obtained from 0.2 mg/mL Keggin-TOF₄ solutions with solvent combinations of (b) 60% water/MeCN, (c) 70% water/MeCN, and (d) 85% water/MeCN. (e) Relationship between the radius of onion-like vesicles and their layer number. (f) Cryo-TEM image of an onion-like vesicle.

on the formation of onion-like vesicles because they provide strong attraction between bilayers. To confirm this, another similar hybrid has been studied: DC_{60} – TOF_4 (Figure S19, synthesis reported in previous work⁴⁸). DC_{60} – TOF_4 has identical rod length and T-shaped architecture to Keggin– TOF_4 , with the only difference being the uncharged DC_{60} clusters (with –OH groups on the surface). In selective solvents, only hollow vesicles are observed in DC_{60} – TOF_4 solutions (Figures S20–S22), suggesting the important roles of counterion-mediated attraction for layer-by-layer assembly of onion-like vesicles.

Coarse-grained (CG) simulation was further applied to further understand the self-assembly behavior at the molecular level. 63-65 In CG simulation, several critical steps during the self-assembly process are observed. Initially, the OF rods strongly interact with each other and attract several hybrids to form the basic building blocks of bilayers (Figure 3e), which aims to minimize the contact areas between hydrophobic OFs and polar solvents. These building blocks further merge together driven by the hydrophobic interaction from OFs (Figure 3f). Due to size disparity between Keggins and OFs, the hybrids tend to form interdigitation to achieve compact packing and meanwhile create curved bilayers (Figure 3g). At this stage, the size of the bilayers is too small to form layer-bylayer attraction with others. With the growth of bilayers, the larger bilayer surface area can enhance counterion-mediated attraction as a glue for layer-by-layer assembly (Figure 3h).

Control of Vesicle Size and Layer Number by Multiple Solution Conditions. The observation of complete onion-like vesicles suggests that the Keggin– TOF_4 hybrids can tolerate a broad range of curvatures, which should not be attributed to their molecular flexibility, as the hybrids are quite rigid. Based on the interdigitation model, the curvature change of bilayers can be achieved by tuning the angle (θ) between adjacent TOF_4 rods (Figure 5d). This process depends on the

supramolecular arrangements of hybrid molecules and thus is controlled by different physical interactions. By adjusting solution conditions to change the strength of physical interactions, ⁶⁶ we could control the supramolecular arrangements between hybrids as well as the curvatures/sizes of bilayers.

Solutions of Keggin-TOF₄ were first prepared in various water/MeCN mixed solvents to study the effects of solvent polarity. As observed from the DLS results, the R_h values of assemblies decrease from 65 ± 5 nm to 35 ± 2 , 26 ± 4 , and 19 \pm 4 nm when the water content (solvent polarity) increases from 50% to 60%, 70%, and 85%, respectively (Figure 4a). All CONTIN curves show a narrow size distribution, suggesting that the vesicle size (i.e., the number of layers) can be well controlled by solvent polarity, and interestingly vesicles tend to grow bigger with more layers in better solvents. This is quite different from the common behavior of typical amphiphiles such as block copolymers. In a solution of typical amphiphiles, the size of assemblies is expected to become larger in a poorer solvent. Meanwhile, the change of solvent polarity will also induce phase transition to various morphologies. 42 The Keggin-TOF₄, on the other hand, exhibits the same selfassembled morphology throughout different solvent polarities. The detailed reason is unclear, but we speculate that it might be related to the rigid structure of TOF4 and their strong interdigitations; that is, the rigid rods tend to interpenetrate with each other more strongly in a poor solvent, preventing the growth of the outer layer in vesicles. The scattered intensities (extrapolated to zero scattered angle) from 50%, 70%, and 85% water/MeCN solutions are 43 000, 4900, and 3350 Kcps, respectively (for benzene: 20 Kcps). Based on the simplified Rayleigh–Gans–Debye equation for solid spheres, 55 $I \propto CM_{\rm w}$ = CR_h^3 , where I is the total scattered intensity and C and M_w are the weight concentration and the mass of the assemblies, respectively. It can be estimated that the weight concentration

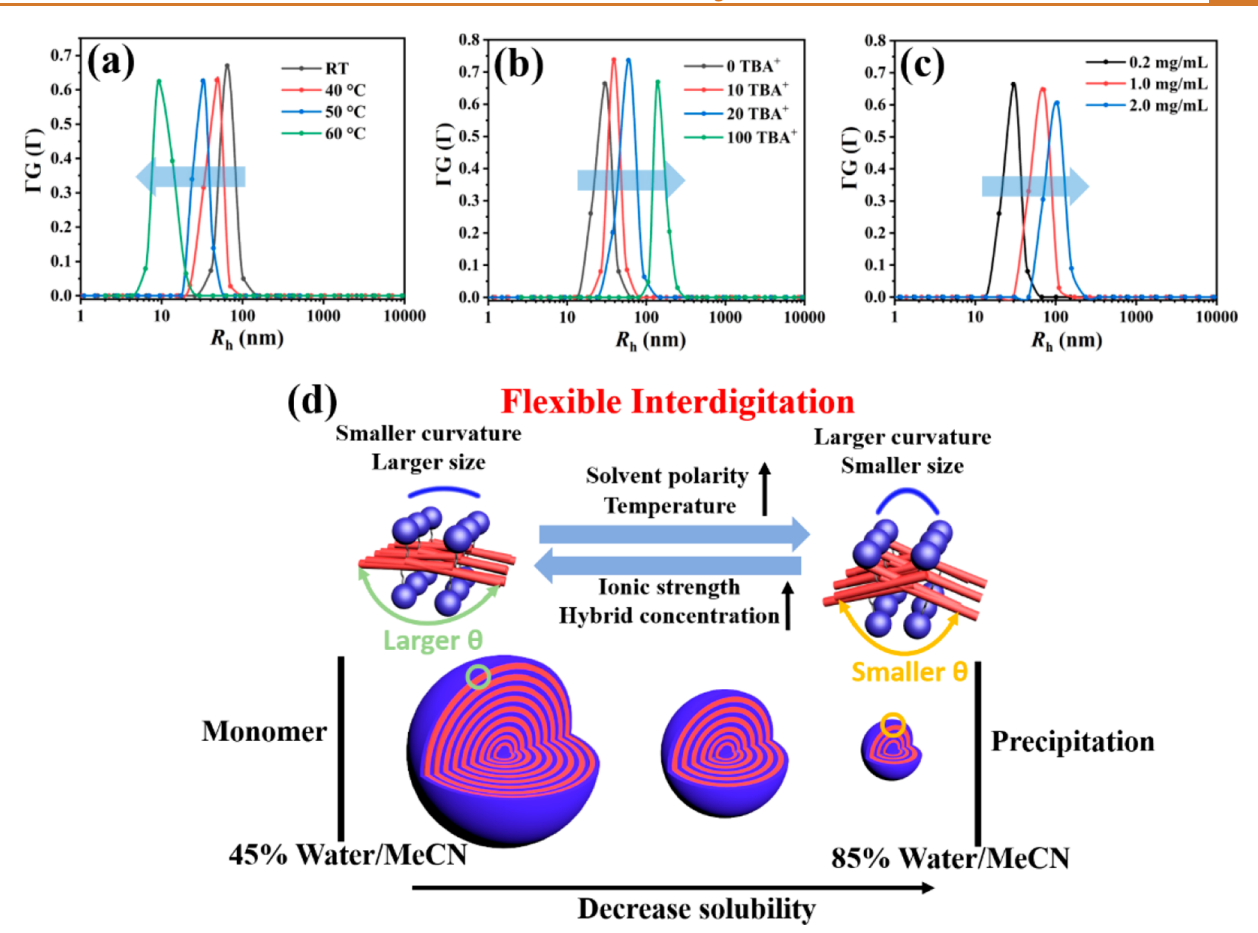


Figure 5. (a) DLS results of 0.2 mg/mL Keggin-TOF₄ (50% water/MeCN) prepared under different temperatures. (b) DLS results of 0.2 mg/mL Keggin-TOF₄ (70% water/MeCN) prepared with addition of different TBA⁺ amounts. (c) DLS results of Keggin-TOF₄ (70% water/MeCN) prepared under different hybrid concentrations. (d) Schematic illustration to show the change of interdigitation between hybrid molecules responsive to different solvent conditions and its effects on the growth of onion-like vesicles. The zoomed-in cartoons of light green and orange circles show the detailed packing of Keggin-TOF₄ at the outermost layer.

of assemblies in 70% and 85% water/MeCN is 1.8 and 3.1 times that in 50% water/MeCN (same sample concentration, 0.2 mg/mL). This suggests that more hybrid molecules will self-assemble into onion-like vesicles at higher solvent polarity, consistent with the fact that Keggin– TOF_4 is less soluble in solutions with higher water contents.

TEM studies further confirm our conclusions. By increasing the water content from 50% to 60%, 70%, and 85%, TEM images show that the average radius of vesicles changes from 61 ± 7 nm (Figure 2c) to 32 ± 5 nm (Figure 4b), 23 ± 2 nm (Figure 4c), and 15 ± 3 nm (Figure 4d), respectively, fully consistent with the DLS measurements. All vesicles observed from TEM possess well-defined onion-like structures. Surprisingly, the average number of layers calculated from TEM exhibits a very good linear relationship with the vesicle size (Figure 4e, detailed analysis in Figures S28-S33). This feature highlights the advantages of the current system because it enables us to precisely manipulate the layer number of onionlike vesicles through controlling physical interactions in solutions. The slope (radius/layer number) from linear fitting is 4.8 nm/layer, in good agreement with the calculated value for the thickness of one bilayer (4.6 nm). Small-angle X-ray scattering (SAXS) measurements of onion-like solutions show an inter-bilayer distance of 5.2 nm (Figure S34), which is close to the slope calculated in Figure 4e. Meanwhile, the interbilayer distance from cryo-TEM is 5.1 ± 0.2 nm (Figure 4f),

very close to the one obtained from regular TEM images; the slight difference in the inter-bilayer distance between cryo-TEM and regular TEM is likely due to the shrinkage during the drying process.

The onion-like vesicles are formed through layer-by-layer self-assembly from inner to outer layers; therefore, the size of vesicles/layer number is determined by growth of the most outside layer. In a given solution condition, the onion-like vesicles will stop growing when different forces are balanced in the outermost layer. From the molecular structure of Keggin-TOF₄, the self-assembly process is expected to be driven by both counterion-mediated electrostatic attraction (from charged Keggins) and hydrophobic interaction (from TOF₄ rods). With increasing solvent polarity, the hydrophobic interaction becomes much stronger, while the strength of counterion-mediated attraction decreases because the Keggins carry more charges. 39,67,68 Overall, the forces between TOF₄ rods become more attractive, while the forces between Keggins become more repulsive, which consequently prefer the interdigitation to smaller angle (θ) and larger curvature (shown in Figure 5d). Therefore, in a more polar solvent, the growth of onion-like vesicles will be limited to the bilayers with larger curvature, that is, onion-like vesicles with smaller

Solvent polarity will simultaneously affect the hydrophobic interaction and counterion-mediated attraction, leading to

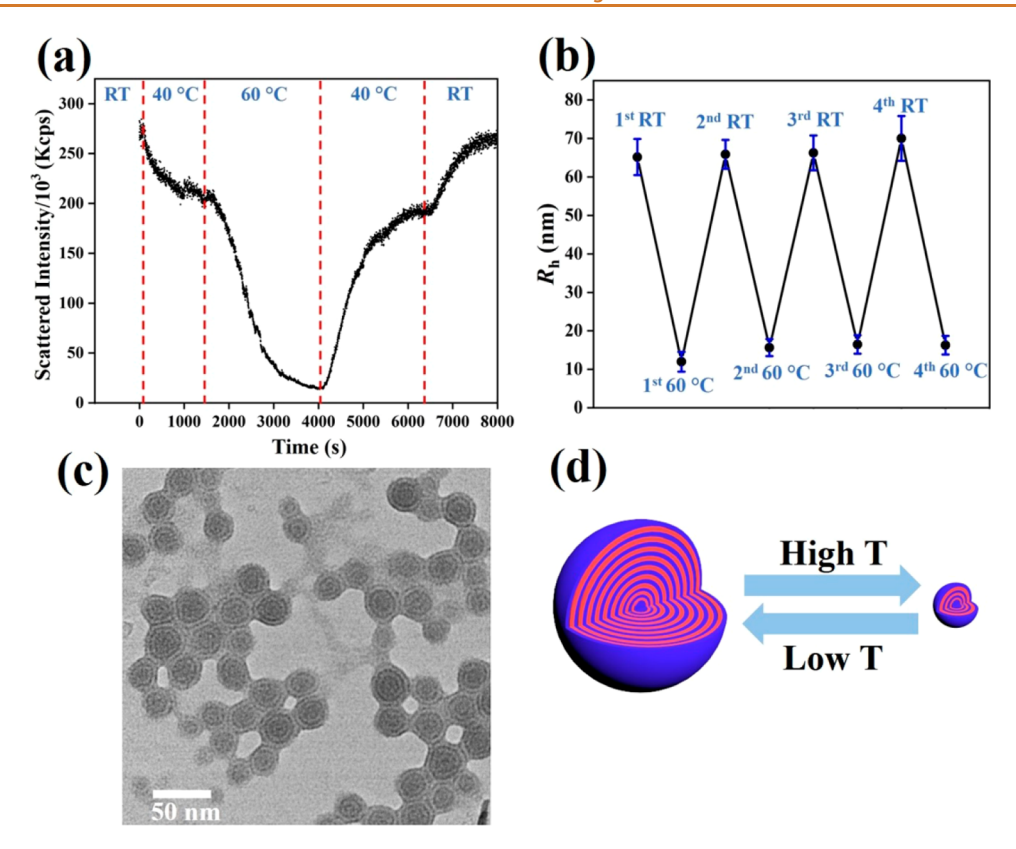


Figure 6. (a) Time-resolved SLS results monitored from 0.2 mg/mL Keggin-TOF $_4$ (50% water/MeCN) solutions with the change of temperature. (b) Reversible response of $R_{\rm h}$ in 0.2 mg/mL Keggin-TOF $_4$ (50% water/MeCN) solutions when repeatedly heating and cooling the sample solutions. (c) TEM images from 0.2 mg/mL Keggin-KOF $_4$ (50% water/MeCN) solutions at 60 °C. (d) Model showing the reversible transformation of onion-like vesicles responsive to temperature changes.

complicated competition between two physical interactions. To simplify the current system as well as re-examine the roles of different interactions, temperature, counterion concentration, and hybrid concentration are applied as extra solution stimuli, aiming for changing the hydrophobic interaction and counterion-mediated attraction, respectively. It is noted that increasing temperature or solvent polarity can both significantly strengthen the hydrophobic interaction,66 while the response of counterion-mediated attraction to temperature is negligible. Indeed, DLS results of sample solutions prepared under different temperatures (Figure 5a) also show a trend of decreasing assembly size (R_h) responsive to the increase of temperature, which are like the effects of increasing solvent polarity. Compared with the TEM image taken from the solutions at room temperature (Figure 2c), the image from higher temperature solutions (Figure 6c) shows that the onionlike vesicles are smaller with fewer layers.

Unlike the temperature effect, the counterion concentration will mostly change the strength of counterion-mediated attraction rather than the hydrophobic interaction. 41,69,70 Meanwhile, higher hybrid concentration will increase the overall ionic strength (TBA+) in solution. From DLS results (Figure 5b and c), the vesicle size becomes larger by increasing the concentration of TBA counterions and Keggin–TOF₄ hybrids. TEM images show that the onion-like vesicles become bigger with more added TBAs or higher hybrid concentration (Figures S23–S26). However, polydispersity starts to appear when the onion-like vesicles further grow larger ($R_{\rm h} > 100$ nm). In solutions with higher ionic strength, the counterion-mediated attraction will be significantly enhanced, the same as

the situation in which the hydrophobic interaction is weakened by considering the competition between two interactions. Consequently, the interdigitation shifts to a higher angle (θ) , shown in Figure 5d, leading to the growth of onion-like vesicles with a smaller curvature (a larger size).

Reversible Transformation of Onion-like Vesicles. Compared with the chain-bending approach by using soft amphiphiles, the rigid sphere-rod shaped hybrids can undergo curvature change by only tuning the degree of interdigitation. The change of interdigitation is controlled by physical interactions and therefore requires less energy than the distortion of chemical bonds in the chain-bending process. This leads to the consequence that the onion-like vesicles might be reversibly transformed due to the low energy barrier of interdigitation. For 0.2 mg/mL Keggin-TOF₄ in 50% water/MeCN solutions prepared at room temperature, they are heated and monitored by time-resolved SLS. The scattered intensity exhibits an obvious drop when raising the temperature from room temperature (RT) to 40 °C, and a more significant drop of intensity is recorded at 60 °C (Figure 6a). Based on the simplified Rayleigh-Gans-Debye equation, the scattered intensity of assemblies is mainly determined by their size (R_h) . DLS measurements show that the R_h of vesicles decreases from 65 nm at RT to 51 nm at 40 °C (Figure 5a) and 12 nm (2.6 layers in Figure 6c) at 60 °C, which consequently leads to a continuous drop of scattered intensity. Combining DLS and SLS results, the weight concentration of assemblies at 60 °C is ca. 5.5 times that at RT, indicating that more hybrids will self-assemble into onion-like vesicles due to the considerable enhancement of hydrophobic interactions at

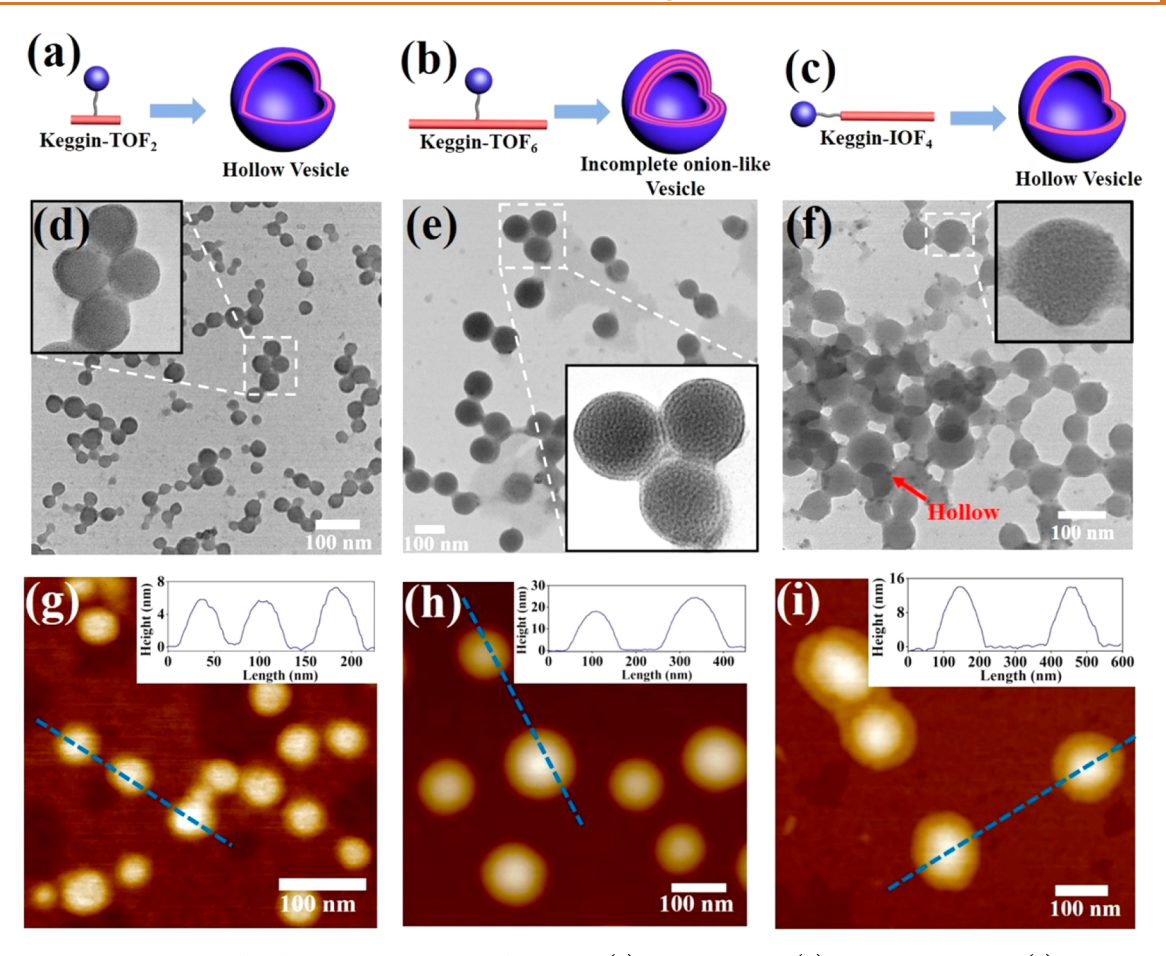


Figure 7. Schematic illustrations of self-assembled structures formed by (a) Keggin–TOF₂, (b) Keggin–TOF₆, and (c) Keggin–IOF₄. TEM images obtained from (d) Keggin–TOF₂, (e) Keggin–TOF₆, and (e) Keggin–IOF₄ solutions with the conditions of 0.2 mg/mL, 50% water/MeCN. AFM images and height profile obtained from (g) Keggin–TOF₂, (h) Keggin–TOF₆, and (e) Keggin–IOF₄ solutions with the conditions of 0.2 mg/mL, 50% water/MeCN.

higher temperatures. Interestingly, the scattered intensity of the solution can return to the original level when cooling the solutions (Figure 6a), suggesting a highly reversible transformation of onion-like vesicles. Indeed, DLS measurements show that the size $(R_{\rm h})$ of vesicles can reversibly respond to the temperature change during heating and cooling processes (Figure 6b).

Effect of Rod Length and Hybrid Architecture. The freedom to change the interdigitation between OF rods comes from their special geometry. In other words, compared with other molecular shapes such as spheres and random coils, the OF rods have a much larger aspect ratio of length/width. Therefore, the rod length should play an important role in the solution behavior of sphere-rod hybrids. A shorter length might make the OF rods behave like spheres and random coils, which accordingly reduce the possibility of forming flexible interdigitation. Three hybrids with the same T-shaped molecular architecture but different rod lengths, Keggin-TOF₂, Keggin-TOF₆, and Keggin-TOF₈, are studied under the same conditions (0.2 mg/mL, 50% water/MeCN). DLS results from Keggin-TOF₂ solution (Figure S35) show that the R_h of the assemblies is 25 nm with a polydispersity, which is consistent with the TEM observations (Figure 7d). A zoomed-in TEM image reveals that the assemblies have no onion-like structures. From AFM measurements (Figure 7g), the average height of the spheres is 6.8 nm, close to the theoretical thickness for collapsed hollow vesicles (9.2 nm). In

UV-vis studies (Figure S36), the absorbance peaks from the OF2 rods have no obvious shift after self-assembly. This indicates that the OF2 rods are not significantly interdigitated during self-assembly, likely due to their short rod length. Accordingly, Keggin-TOF2 cannot achieve different curvatures in bilayers and can only form regular hollow vesicles. Meanwhile, self-assembly can also be observed in the solutions of Keggin-TOF₆ by forming 60-nm-radius spherical structures (Figure S37), and TEM images (Figure 7e) show spherical assemblies with similar size. Longer rod length is expected to enhance the possibility of flexible interdigitation, which in turn favors the formation of onion-like vesicles. However, a zoomed-in TEM image shows that the vesicles have only a few outer layers rather than complete onions. From AFM measurements (Figure 7h), the height of vesicles ranges from 16 to 26 nm, which is roughly the thickness of 2 or 3 bilayers based on the molecular structure of Keggin-TOF₆. Due to their longer rod length, it might be difficult to fit long OF rods into the hydrophobic domains of bilayers due to space restriction (especially for the inner layers). Accordingly, the Keggin-TOF₆ cannot form complete onion-like vesicles. By further increasing the rod length to Keggin-TOF8, the hydrophobic parts become so dominant that only irregular precipitates are observed (Figure S38).

In addition to the rod length, hybrids with different architectures (Keggin–IOF₄ in Figure 7c) are also studied. $R_h = 53$ nm (Figure S39) spherical assemblies are observed

which do not show onion-like structures (Figure 7f). Moreover, the shape of one sphere can be clearly observed with the presence of another sphere on the top, indicating that the spheres possess the feature of a thin layer after collapse (hollow spheres). This is also confirmed by AFM measurements, with an average height of collapsed spheres being 14.3 nm (Figure 7i), in agreement with the value for hollow vesicle (20.4 nm). In the T-shaped hybrid architecture (Keggin-TOF₄), the TOF₄ rods pack perpendicular to Keggins in bilayers, and the change of interdigitation will not significantly affect the distance between Keggin clusters (Figure 5d). However, the IOF4 rods are expected to pack parallel to Keggins in the case of Keggin-IOF₄. Consequently, the distance between Keggins will be dramatically changed when the angle between IOF₄ rods is tuned (Figure S41), leading to unstable packing of the bilayer structure because the counterion-mediated attraction is sensitive to intermolecular distance. Therefore, the Keggin-IOF₄ prefers to form regular hollow vesicles rather than onion-like vesicles.

CONCLUSION

We report a mechanism for the formation of onion-like vesicles. The onion-like vesicles are highly controllable, uniform, and responsive and are observed in polar solvents of the sphere-rod shaped hybrid (Keggin-TOF₄) via the flexible interdigitation of TOF4 rods. The interdigitation degree can be regulated by solution conditions including solvent polarity, temperature, counterion concentration, and hybrid concentration. The change of interdigitation affects the bilayer curvature and leads to the formation of onion-like vesicles, which can be manipulated by multiple solution conditions. The size and the layer number of onion-like vesicles exhibit a good linear relationship with a fixed interlayer distance. The vesicle size/layer number can reversibly respond to the change of temperature. The charged Keggin clusters show an important role by providing strong counterionmediated attraction between bilayers. Moreover, the rod length and hybrid architecture have significant effects on the formation of onion-like vesicles. This study provides a fundamental understanding for the self-assembly of onionlike vesicles by amphiphilic molecules and might lead to possible opportunity for programmable self-assembly of amphiphiles into onion-like vesicles due to their highly controllable and responsive properties. The onion-like vesicle formation suggests potentially rich, uncharted self-assembly behaviors of rigid amphiphilic materials in dilute solution.

METHODS

Dynamic Light Scattering and Static Light Scattering. Both DLS and SLS measurements were performed on a Brookhaven Instruments light scattering spectrometer equipped with a diodepumped solid-state laser operating at 532 nm and a BI-9000AT multichannel digital correlator. The SLS was performed over a broad range of scattered angles from 30° to 90°, with 2° intervals. The radius of gyration (R_{σ}) was calculated by using a partial Zimm plot derived from the Rayleigh-Gans-Debye equation. The partial Zimm plot was obtained from the following approximate formula: 1/I = C(1 $+R_{\rm g}^2q^2/3$). The $R_{\rm g}$ was determined from the slope and intercept of a plot of $1/I vs q^2$. For DLS measurements, the intensity—intensity time correlation functions were analyzed by the constrained regularized (CONTIN) method. The average apparent translational diffusion coefficient, $D_{\rm app}$, was determined from the normalized distribution function of the characteristic line width, $\Gamma(G)$. The hydrodynamic radius (R_h) was converted from D through the Stokes-Einstein

equation: $R_{\rm h} = KT/6\pi\eta D$, where K is the Boltzmann constant and η is the viscosity of the solvent at temperature T. The temperature of the chamber in the light scattering equipment was controlled by a circulating bath with an accuracy of 0.1 °C.

Nuclear Magnetic Resonance. Both 1D and 2D NMR spectra were measured on a Varian NMRS 500 spectrometer equipped with a 5 mm dual broadband probe. 2D NOESY measurements were recorded with 256 t1 increments and 32 scans, with a relaxation time of 2 s. The mixing time changed from 0.2 s to 0.5 s. Baseline and phase correction were performed when appropriate.

Transmission Electron Microscopy. Regular TEM images were taken on a JEOL JEM-1230 electron microscope operated at 120 kV. Samples for regular TEM analysis were prepared by dropping a small volume of solution on a copper grid and fast drying under an oil pump. To improve the visibility of onion-like vesicles, the contrast and brightness of TEM images were enhanced. Cryogenic transmission electron microscopy (cryo-TEM) specimens were prepared by using a FEI Vitrobot (Mark IV) plunge freezer to prepare vitrified cryo-TEM specimens. A 3 μ L amount of the solution was applied to a TEM grid coated with a lacey carbon film. After blotting using two filter papers, the grid was plunge-frozen in liquid ethane. The vitrified specimen was mounted onto a Gatan 626.DH cryo-TEM holder and transferred into a FEI Tecnai F20 TEM equipped with a Gatan twin blade retractable anticontaminator. The cryo-TEM observation was carried out at \sim -174 °C. The basic experimental setup and procedure can be found in ref 71.

Atomic Force Microscopy. AFM measurements were conducted a Dimension Icon AFM (Bruker AXS). Samples were prepared by drop-casting a 20 μ L solution onto the silica substrates. After evaporation of the solvent, images were taken in the soft tapping mode at a resolution of 512 \times 512 pixel per image. Data analyses were performed using NanoScope Analysis 1.5 software.

Matrix-Assisted Laser Desorption/Ionization Time-of-Flight Mass Spectroscopy. MALDI-TOF mass spectra were measured on a Bruker Ultraflex III TOF/TOF mass spectrometer (Bruker Daltonics). trans-2-[3-(4-tert-Butylphenyl)-2-methyl-2-propenylidene] malononitrile (DCTB) was used as matrix compound. Tetrabutylammonium bromide (TBABr) was used as ionizing agent. The sample was prepared by depositing 0.5 μ L of matrix solution on the wells of a 384-well ground-steel plate and depositing 0.5 μ L of sample solution on a spot of dried matrix, then adding another 0.5 μ L of matrix solution on top of the dried sample. Mass spectra were measured in the reflection mode, and the mass scale was calibrated externally with PS standards with similar molecular weights to those of the samples under consideration. Data analyses were conducted with Bruker's Flex Analysis software.

Small-Angle X-ray Scattering. In order to carry out SAXS measurement, a Keggin— TOF_4 solution containing onion-like vesicles was loaded in quartz capillary tubes of 1.5 mm diameter. SAXS measurement was carried at the SAXS instrument of NSF's ChemMatCARS (15-ID-D station) at the Advanced Photon Source. The measurement was done with X-rays of energy 13.474 keV with a sample to detector distance of 0.58 m. A direct photon counting pixel area detector, Pilatus3 X 300K, from DECTRIS was used for obtaining the SAXS pattern from the sample.

Wide-Angle X-ray Scattering (WAXS). WAXS experiments were carried out on a Rigaku 18 kW rotating anode generator equipped with an image plate as the detector. The instrument was calibrated using silicon powders with 2θ being 28.4° under Cu K α radiation.

Fourier-Transform Infrared Spectroscopy. Infrared spectra were measured on a PerkinElmer FTIR spectrometer.

Sample Preparation. Typically, the solid samples were dissolved in acetonitrile. The solutions were passed through a PTFE syringe filter with 200 nm pore size. The acetonitrile sample solutions were loaded into a 20 mL vial; then additional acetonitrile and water were slowly added with stirring to adjust the solution parameters.

ASSOCIATED CONTENT

Supporting Information

The Supporting Information is available free of charge at https://pubs.acs.org/doi/10.1021/acsnano.9b07611.

Simulation details, synthetic procedures, NMR, UV-vis, MALDI-TOF MS, and FTIR characterizations of final products and SAXS, WAXS, DLS, SLS, and TEM results (PDF)

AUTHOR INFORMATION

Corresponding Authors

Stephen Z. D. Cheng – Department of Polymer Science, The University of Akron, Akron, Ohio 44325, United States; South China Advanced Institute for Soft Matter Science and Technology, South China University of Technology, Guangzhou 510640, China;

orcid.org/0000-0003-1448-0546; Email: scheng@uakron.edu

Tianbo Liu – Department of Polymer Science, The University of Akron, Akron, Ohio 44325, United States; oorcid.org/0000-0002-8181-1790; Email: tliu@uakron.edu

Jiancheng Luo – Department of Polymer Science, The University of Akron, Akron, Ohio 44325, United States; oorcid.org/0000-0002-3766-4922

Tong Liu – Department of Polymer Science, The University of Akron, Akron, Ohio 44325, United States; South China Advanced Institute for Soft Matter Science and Technology and School of Molecular Science and Engineering, South China University of Technology, Guangzhou 510640, China

Kun Qian - Department of Polymer Science, The University of Akron, Akron, Ohio 44325, United States

Benqian Wei - Department of Polymer Science, The University of Akron, Akron, Ohio 44325, United States

Yinghe Hu – Department of Polymer Science, The University of Akron, Akron, Ohio 44325, United States

Min Gao - Advanced Materials and Liquid Crystal Institute, Kent State University, Kent, Ohio 44242, United States

Xinyu Sun - Department of Polymer Science, The University of Akron, Akron, Ohio 44325, United States; oorcid.org/0000-0003-4353-1832

Zhiwei Lin – Department of Polymer Science, The University of Akron, Akron, Ohio 44325, United States

Jiahui Chen – Department of Polymer Science, The University of Akron, Akron, Ohio 44325, United States; oorcid.org/0000-0002-3861-146X

Mrinal K. Bera - NSF's ChemMatCARS, The University of Chicago, Chicago, Illinois 60637, United States

Yuhang Chen – Department of Polymer Science, The University of Akron, Akron, Ohio 44325, United States

Ruimeng Zhang - Department of Polymer Science, The University of Akron, Akron, Ohio 44325, United States

Jialin Mao – Department of Chemistry, The University of Akron, Akron, Ohio 44325, United States; o orcid.org/0000-0002-5011-

Chrys Wesdemiotis – Department of Polymer Science and Department of Chemistry, The University of Akron, Akron, Ohio 44325, United States

Mesfin Tsige - Department of Polymer Science, The University of Akron, Akron, Ohio 44325, United States; o orcid.org/0000-0002-7540-2050

Complete contact information is available at: https://pubs.acs.org/10.1021/acsnano.9b07611

Notes

The authors declare no competing financial interest.

ACKNOWLEDGMENTS

T.L. acknowledges support by National Science Foundation (NSF, CHE1904397) and the University of Akron. S.Z.D.C. acknowledges support by The Pearl River Talent Recruitment Program of Guangdong Province (no. 2016ZT06C322) and National Natural Science Foundation of China (U1832220). K.Q. and M.T. acknowledge support from NSF (CHE-1665284). C.W. acknowledges support from NSF (CHE-1808115). The cryo-TEM experiment was carried out at the Characterization Facility of Advanced Materials and Liquid Crystal Institute of Kent State University. NSF's ChemMat-CARS Sector 15 is supported by the Divisions of Chemistry (CHE) and Materials Research (DMR), National Science Foundation, under grant number NSF/CHE-1834750. Use of the Advanced Photon Source, an Office of Science User Facility operated for the U.S. Department of Energy (DOE) Office of Science by Argonne National Laboratory, was supported by the U.S. DOE under Contract No. DE-AC02-06CH11357. We thank Dr. Wenpeng Shan for helpful discussions, Dr. Hao Liu for providing a 3D model of onionlike vesicles, and Dr. Zhuonan Liu for building up the CG model of Keggin macroions.

REFERENCES

- (1) Discher, D. E.; Eisenberg, A. Polymer Vesicles. Science 2002, 297, 967-973.
- (2) Torchilin, V.; Weissig, V. Liposomes: A Practical Approach; Oxford University Press: Oxford, 2003.
- (3) Antonietti, M.; Förster, S. Vesicles and Liposomes: A Self-Assembly Principle Beyond Lipids. Adv. Mater. 2003, 15, 1323-1333.
- (4) Israelachvili, J. N.; Mitchell, D. J.; Ninham, B. W.; Physics, C. Theory of Self-Assembly of Hydrocarbon Amphiphiles into Micelles and Bilayers. J. Chem. Soc., Faraday Trans. 2 1976, 72, 1525-1568.
- (5) Percec, V.; Wilson, D. A.; Leowanawat, P.; Wilson, C. J.; Hughes, A. D.; Kaucher, M. S.; Hammer, D. A.; Levine, D. H.; Kim, A. J.; Bates, F. S.; Davis, K. P.; Lodge, T. P.; Klein, M. L.; DeVane, R. H.; Aqad, E.; Rosen, B. M.; Argintaru, A. O.; Sienkowska, M. J.; Rissanen, K.; Nummelin, S.; et al. Self-Assembly of Janus Dendrimers into Uniform Dendrimersomes and Other Complex Architectures. Science 2010, 328, 1009-1014.
- (6) Zhang, X.; Wang, C. Supramolecular Amphiphiles. Chem. Soc. Rev. 2011, 40, 94-101.
- (7) Rosen, B. M.; Wilson, D. A.; Wilson, C. J.; Peterca, M.; Won, B. C.; Huang, C.; Lipski, L. R.; Zeng, X.; Ungar, G.; Heiney, P. A.; Percec, V. Predicting the Structure of Supramolecular Dendrimers via the Analysis of Libraries of AB3 and Constitutional Isomeric AB2 Biphenylpropyl Ether Self-Assembling Dendrons. J. Am. Chem. Soc. 2009, 131, 17500-17521.
- (8) Elani, Y.; Law, R. V.; Ces, O. Vesicle-Based Artificial Cells as Chemical Microreactors with Spatially Segregated Reaction Pathways. Nat. Commun. 2014, 5, 5305.
- (9) Maiti, S.; Fortunati, I.; Ferrante, C.; Scrimin, P.; Prins, L. J. Dissipative Self-Assembly of Vesicular Nanoreactors. Nat. Chem. **2016**, 8, 725–731.
- (10) Ruan, G.; Agrawal, A.; Marcus, A. I.; Nie, S. Imaging and Tracking of Tat Peptide-Conjugated Quantum Dots in Living Cells: New Insights into Nanoparticle Uptake, Intracellular Transport, and Vesicle Shedding. J. Am. Chem. Soc. 2007, 129, 14759-14766.
- (11) Noguchi, H.; Takasu, M. Self-Assembly of Amphiphiles into Vesicles: A Brownian Dynamics Simulation. Phys. Rev. E: Stat. Phys., Plasmas, Fluids, Relat. Interdiscip. Top. 2001, 64, 041913.

- (12) Marrink, S. J.; Mark, A. E. The Mechanism of Vesicle Fusion as Revealed by Molecular Dynamics Simulations. *J. Am. Chem. Soc.* **2003**, *125*, 11144–11145.
- (13) Sevink, G.; Zvelindovsky, A. Self-Assembly of Complex Vesicles. *Macromolecules* **2005**, 38, 7502–7513.
- (14) Gulik-Krzywicki, T.; Dedieu, J.; Roux, D.; Degert, C.; Laversanne, R. Freeze-Fracture Electron Microscopy of Sheared Lamellar Phase. *Langmuir* **1996**, *12*, 4668–4671.
- (15) Song, A.; Dong, S.; Jia, X.; Hao, J.; Liu, W.; Liu, T. An Onion Phase in Salt-Free Zero-Charged Catanionic Surfactant Solutions. *Angew. Chem., Int. Ed.* **2005**, *44*, 4018–4021.
- (16) Dong, R.; Zhong, Z.; Hao, J. Self-Assembly of Onion-Like Vesicles Induced by Charge and Rheological Properties in Anionic—Nonionic Surfactant Solutions. *Soft Matter* **2012**, *8*, 7812—7821.
- (17) Li, L.; Rosenthal, M.; Zhang, H.; Hernandez, J. J.; Drechsler, M.; Phan, K. H.; Rütten, S.; Zhu, X.; Ivanov, D. A.; Möller, M. Light-Switchable Vesicles from Liquid-Crystalline Homopolymer-Surfactant Complexes. *Angew. Chem., Int. Ed.* **2012**, *51*, 11616–11619.
- (18) Shen, H.; Eisenberg, A. Control of Architecture in Block-Copolymer Cesicles. *Angew. Chem., Int. Ed.* **2000**, *39*, 3310–3312.
- (19) Li, C.; Yan, J.; Hu, X.; Liu, T.; Sun, C.; Xiao, S.; Yuan, J.; Chen, P.; Zhou, S. Conductive Polyaniline Helixes Self-Assembled in the Absence of Chiral Dopant. *Chem. Commun.* **2013**, *49*, 1100–1102.
- (20) Fan, H.; Jin, Z. Freezing Polystyrene-b-Poly (2-Vinylpyridine) Micelle Nanoparticles with Different Nanostructures and Sizes. *Soft Matter* **2014**, *10*, 2848–2855.
- (21) Klinger, D.; Wang, C. X.; Connal, L. A.; Audus, D. J.; Jang, S. G.; Kraemer, S.; Killops, K. L.; Fredrickson, G. H.; Kramer, E. J.; Hawker, C. J. A Facile Synthesis of Dynamic, Shape-Changing Polymer Particles. *Angew. Chem., Int. Ed.* **2014**, *53*, 7018–7022.
- (22) Zhang, S.; Sun, H.-J.; Hughes, A. D.; Moussodia, R.-O.; Bertin, A.; Chen, Y.; Pochan, D. J.; Heiney, P. A.; Klein, M. L.; Percec, V. Self-Assembly of Amphiphilic Janus Dendrimers into Uniform Onion-Like Dendrimersomes with Predictable Size and Number of Bilayers. *Proc. Natl. Acad. Sci. U. S. A.* **2014**, *111*, 9058–9063.
- (23) Xiao, Q.; Sherman, S. E.; Wilner, S. E.; Zhou, X.; Dazen, C.; Baumgart, T.; Reed, E. H.; Hammer, D. A.; Shinoda, W.; Klein, M. L.; Percec, V. Janus Dendrimersomes Coassembled from Fluorinated, Hydrogenated, and Hybrid Janus Dendrimers as Models for Cell Fusion and Fission. *Proc. Natl. Acad. Sci. U. S. A.* 2017, 114, E7045.
- (24) Peterca, M.; Percec, V.; Leowanawat, P.; Bertin, A. Predicting the Size and Properties of Dendrimersomes from the Lamellar Structure of Their Amphiphilic Janus Dendrimers. *J. Am. Chem. Soc.* **2011**, 133, 20507–20520.
- (25) Sherman, S. E.; Xiao, Q.; Percec, V. Mimicking Complex Biological Membranes and Their Programmable Glycan Ligands with Dendrimersomes and Glycodendrimersomes. *Chem. Rev.* **2017**, *117*, 6538–6631.
- (26) Xiao, Q.; Zhang, S.; Wang, Z.; Sherman, S. E.; Moussodia, R.-O.; Peterca, M.; Muncan, A.; Williams, D. R.; Hammer, D. A.; Vértesy, S.; André, S.; Gabius, H.-J.; Klein, M. L.; Percec, V. Onion-Like Glycodendrimersomes from Sequence-Defined Janus Glycodendrimers and Influence of Architecture on Reactivity to ALectin. *Proc. Natl. Acad. Sci. U. S. A.* **2016**, *113*, 1162.
- (27) Torre, P.; Xiao, Q.; Buzzacchera, I.; Sherman, S. E.; Rahimi, K.; Kostina, N. Y.; Rodriguez-Emmenegger, C.; Möller, M.; Wilson, C. J.; Klein, M. L.; Good, M. C.; Percec, V. Encapsulation of Hydrophobic Components in Dendrimersomes and Decoration of Their Surface with Proteins and Nucleic Acids. *Proc. Natl. Acad. Sci. U. S. A.* **2019**, *116*, 15378.
- (28) Li, H.; Sun, H.; Qi, W.; Xu, M.; Wu, L. Onionlike Hybrid Assemblies Based on Surfactant-Encapsulated Polyoxometalates. *Angew. Chem., Int. Ed.* **2007**, *46*, 1300–1303.
- (29) Burger, C.; Hao, J.; Ying, Q.; Isobe, H.; Sawamura, M.; Nakamura, E.; Chu, B. Multilayer Vesicles and Vesicle Clusters Formed by the Fullerene-Based Surfactant C60(CH3)5K. J. Colloid Interface Sci. 2004, 275, 632–641.

- (30) Landsmann, S.; Luka, M.; Polarz, S. Bolaform Surfactants with Polyoxometalate Head Groups and Their Assembly into Ultra-Small Monolayer Membrane Vesicles. *Nat. Commun.* **2012**, *3*, 1299.
- (31) Liu, H.; Luo, J.; Shan, W.; Guo, D.; Wang, J.; Hsu, C.-H.; Huang, M.; Zhang, W.; Lotz, B.; Zhang, W.-B.; Liu, T.; Yue, K.; Cheng, S. Z. D. Manipulation of Self-Assembled Nanostructure Dimensions in Molecular Janus Particles. *ACS Nano* **2016**, *10*, 6585–6596
- (32) Zhou, S.; Feng, Y.; Chen, M.; Li, Q.; Liu, B.; Cao, J.; Sun, X.; Li, H.; Hao, J. Robust Onionlike Structures with Magnetic and Photodynamic Properties Formed by A Fullerene C60–POM hybrid. *Chem. Commun.* **2016**, *52*, 12171–12174.
- (33) Wang, H.-Y.; Ren, L.-J.; Wang, X.-G.; Ming, J.-B.; Wang, W. Insights into the Self-Assembly of a Heterocluster Janus Molecule into Colloidal Onions. *Langmuir* **2019**, *35*, 6727–6734.
- (34) Chang, H.-Y.; Lin, Y.-L.; Sheng, Y.-J.; Tsao, H.-K. Structural Characteristics and Fusion Pathways of Onion-Like Multilayered Polymersome Formed by Amphiphilic Comb-Like Graft Copolymers. *Macromolecules* **2013**, *46*, 5644–5656.
- (35) Arai, N.; Yasuoka, K.; Zeng, X. C. Self-Assembly of Janus Oligomers into Onion-Like Vesicles with Layer-By-Layer Water Discharging Capability: A Minimalist Model. *ACS Nano* **2016**, *10*, 8026–8037.
- (36) Jung, H. T.; Coldren, B.; Zasadzinski, J. A.; Iampietro, D. J.; Kaler, E. W. The Origins of Stability of Spontaneous Vesicles. *Proc. Natl. Acad. Sci. U. S. A.* **2001**, 98, 1353.
- (37) Claessens, M. M. A. E.; van Oort, B. F.; Leermakers, F. A. M.; Hoekstra, F. A.; Cohen Stuart, M. A. Charged Lipid Vesicles: Effects of Salts on Bending Rigidity, Stability, and Size. *Biophys. J.* **2004**, *87*, 3882–3893.
- (38) Huang, C.; Quinn, D.; Sadovsky, Y.; Suresh, S.; Hsia, K. J. Formation and Size Distribution of Self-Assembled Vesicles. *Proc. Natl. Acad. Sci. U. S. A.* **2017**, *114*, 2910.
- (39) Luo, J.; Liu, T. Competition and Cooperation among Different Attractive Forces in Solutions of Inorganic—Organic Hybrids Containing Macroionic Clusters. *Langmuir* **2019**, *35*, 7603—7616.
- (40) Yin, P.; Li, D.; Liu, T. Solution Behaviors and Self-Assembly of Polyoxometalates as Models of Macroions and Amphiphilic Polyoxometalate—Organic Hybrids as Novel Surfactants. *Chem. Soc. Rev.* **2012**, *41*, 7368–7383.
- (41) Liu, T. Hydrophilic Macroionic Solutions: What Happens When Soluble Ions Reach the Size of Nanometer Scale? *Langmuir* **2010**, *26*, 9202–9213.
- (42) Mai, Y.; Eisenberg, A. Self-Assembly of Block Copolymers. Chem. Soc. Rev. 2012, 41, 5969–5985.
- (43) Voevodin, A.; Campos, L. M.; Roy, X. Multifunctional Vesicles from a Self-Assembled Cluster-Containing Diblock Copolymer. *J. Am. Chem. Soc.* **2018**, *140*, 5607–5611.
- (44) Chu, Y.; Zhang, W.; Lu, X.; Mu, G.; Zhang, B.; Li, Y.; Cheng, S. Z. D.; Liu, T. Rational Controlled Morphological Transitions in the Self-Assembled Multi-Headed Giant Surfactants in Solution. *Chem. Commun.* **2016**, *52*, 8687–8690.
- (45) Olsen, B. D.; Segalman, R. A. Self-Assembly of Rod-Coil Block Copolymers. *Mater. Sci. Eng., R* **2008**, *62*, 37–66.
- (46) Zhang, J.; Chen, X.-F.; Wei, H.-B.; Wan, X.-H. Tunable Assembly of Amphiphilic Rod-Coil Block Copolymers in Solution. *Chem. Soc. Rev.* **2013**, *42*, 9127–9154.
- (47) Micoine, K.; Hasenknopf, B.; Thorimbert, S.; Lacôte, E.; Malacria, M. A General Strategy for Ligation of Organic and Biological Molecules to Dawson and Keggin Polyoxotungstates. *Org. Lett.* **2007**, *9*, 3981–3984.
- (48) Lin, Z.; Yang, X.; Xu, H.; Sakurai, T.; Matsuda, W.; Seki, S.; Zhou, Y.; Sun, J.; Wu, K.-Y.; Yan, X.-Y.; Zhang, R.; Huang, M.; Mao, J.; Wesdemiotis, C.; Aida, T.; Zhang, W.; Cheng, S. Z. D. Topologically Directed Assemblies of Semiconducting Sphere—Rod Conjugates. J. Am. Chem. Soc. 2017, 139, 18616—18622.
- (49) Zhang, R.; Feng, X.; Zhang, R.; Shan, W.; Su, Z.; Mao, J.; Wesdemiotis, C.; Huang, J.; Yan, X.-Y.; Liu, T.; Li, T.; Huang, M.; Lin, Z.; Shi, A.-C.; Cheng, S. Z. D. Breaking Parallel Orientation of

- Rods via a Dendritic Architecture toward Diverse Supramolecular Structures. Angew. Chem. 2019, 131, 12005–12011.
- (50) Proust, A.; Matt, B.; Villanneau, R.; Guillemot, G.; Gouzerh, P.; Izzet, G. Functionalization and Post-Functionalization: A Step Towards Polyoxometalate-Based Materials. *Chem. Soc. Rev.* **2012**, 41, 7605–7622.
- (51) Dolbecq, A.; Dumas, E.; Mayer, C. R.; Mialane, P. Hybrid Organic-Inorganic Polyoxometalate Compounds: From Structural Diversity to Applications. *Chem. Rev.* **2010**, *110*, 6009–6048.
- (52) Nagarajan, R.; Ruckenstein, E. Theory of Surfactant Self-Assembly: A Predictive Molecular Thermodynamic Approach. *Langmuir* 1991, 7, 2934–2969.
- (53) Zhang, J.; Song, Y.-F.; Cronin, L.; Liu, T. Self-Assembly of Organic-Inorganic Hybrid Amphiphilic Surfactants with Large Polyoxometalates as Polar Head Groups. *J. Am. Chem. Soc.* **2008**, 130, 14408–14409.
- (54) Provencher, S. W. CONTIN: A General Purpose Constrained Regularization Program for Inverting Noisy Linear Algebraic and Integral Equations. *Comput. Phys. Commun.* **1982**, 27, 229–242.
- (55) Hiemenz, P. C. Principles of Colloid and Surface Chemistry; M. Dekker: New York, 1986.
- (56) Discher, B. M.; Hammer, D. A.; Bates, F. S.; Discher, D. E.; Science, I. Polymer Vesicles in Various Media. *Curr. Opin. Colloid Interface Sci.* **2000**, *5*, 125–131.
- (57) Larsen, J.; Hatzakis, N. S.; Stamou, D. Observation of Inhomogeneity in the Lipid Composition of Individual Nanoscale Liposomes. J. Am. Chem. Soc. 2011, 133, 10685–10687.
- (58) Ernst, R. R.; Bodenhausen, G.; Wokaun, A. Principles of Nuclear Magnetic Resonance in One and Two Dimensions; Clarendon Press: Oxford, 1987.
- (59) Denkova, P. S.; Van Lokeren, L.; Willem, R. Mixed Micelles of Triton X-100, Sodium Dodecyl Dioxyethylene Sulfate, and Synperonic l61 Investigated by NOESY and Diffusion Ordered NMR Spectroscopy. *J. Phys. Chem. B* **2009**, *113*, 6703–6709.
- (60) Zhu, L.; Yang, C.; Qin, J. An Aggregation-Induced Blue Shift of Emission and the Self-Assembly of Nanoparticles From A Novel Amphiphilic Oligofluorene. *Chem. Commun.* **2008**, 6303–6305.
- (61) Kuehne, A. J.; Gather, M. C.; Sprakel, J. Monodisperse Conjugated Polymer Particles by Suzuki–Miyaura Dispersion Polymerization. *Nat. Commun.* **2012**, *3*, 1088.
- (62) Liu, G.; Liu, T. Strong Attraction among the Fully Hydrophilic {Mo72Fe30} Macroanions. *J. Am. Chem. Soc.* **2005**, 127, 6942–6943.
- (63) Kremer, K.; Grest, G. S. Dynamics of Entangled Linear Polymer Melts: A Molecular-Dynamics Simulation. *J. Chem. Phys.* **1990**, 92, 5057–5086.
- (64) Liu, Z.; Liu, T.; Tsige, M. Elucidating the Origin of the Attractive Force among Hydrophilic Macroions. *Sci. Rep.* **2016**, *6*, 26595.
- (65) Liu, Z.; Liu, T.; Tsige, M. Unique Symmetry-Breaking Phenomenon during the Self-Assembly of Macroions Elucidated by Simulation. *Sci. Rep.* **2018**, *8*, 13076.
- (66) Israelachvili, J. N. Intermolecular and Surface Forces; Academic Press: Cambridge, 2011.
- (67) Ashbaugh, H. S.; Pratt, L. R. Colloquium: Scaled Particle Theory and the Length Scales of Hydrophobicity. *Rev. Mod. Phys.* **2006**, 78, 159–178.
- (68) Kistler, M. L.; Bhatt, A.; Liu, G.; Casa, D.; Liu, T. A Complete Macroion-"Blackberry" Assembly-Macroion Transition with Continuously Adjustable Assembly Sizes in {Mo132} Water/Acetone Systems. J. Am. Chem. Soc. 2007, 129, 6453–6460.
- (69) Liu, G.; Liu, T. Thermodynamic Properties of the Unique Self-Assembly of {Mo72Fe30} Inorganic Macro-Ions in Salt-Free and Salt-Containing Aqueous Solutions. *Langmuir* **2005**, *21*, 2713–2720.
- (70) Misra, A.; Kozma, K.; Streb, C.; Nyman, M. Beyond Charge Balance: Counter-Cations in Polyoxometalate Chemistry. *Angew. Chem., Int. Ed.* **2020**, *59*, 596–612.
- (71) Gao, M.; Kim, Y.-K.; Zhang, C.; Borshch, V.; Zhou, S.; Park, H.-S.; Jákli, A.; Lavrentovich, O. D.; Tamba, M.-G.; Kohlmeier, A.; Mehl, G. H.; Weissflog, W.; Studer, D.; Zuber, B.; Gnägi, H.; Lin, F.

Direct Observation of Liquid Crystals Using Cryo-TEM: Specimen Preparation and Low-Dose Imaging. *Microsc. Res. Tech.* **2014**, 77, 754–772.